Proceedings of ERAD (2002): 266–271 © Copernicus GmbH 2002

ERAD 2002

An enhanced precipitation accumulation algorithm for radar data

R. Hannesen[1] **and H. Gysi**[2]

[1]Gematronik GmbH Elektronische Anlagen, Raiffeisenstr. 10, 41470 Neuss, Germany
[2]Radar-Info, Roonstr. 18, 76137 Karlsruhe, Germany

Abstract. Conventional precipitation accumulation algorithms for radar data usually add up instantaneous precipitation intensity fields multiplied with the time interval between the data samples. This method does not take into account the propagation and development of the precipitation systems in the time between the data samples. As a consequence, the derived horizontal distribution of precipitation accumulation gives wrong results; in particular for small-scale fast-moving cells, when a clustering appears in the accumulation maps.

This paper presents an algorithm which derives information about precipitation pattern movement and development using different tracking techniques or other radar data sources. The vector field information is used to combine instantaneous precipitation intensity fields of subsequent radar data samples by modelling the precipitation system development between the samples.

The results demonstrate the improvement of the precipitation accumulation fields. In a case study, the results of different techniques are compared with rain gauge measurements. Computation time statistics are given which demonstrate that the different techniques can be used in real-time on standard PC stations.

1 Introduction

Precipitation measurements by means of weather radar has become an important method during the past decades. Corrections for several inaccuracies in the measurement of precipitation intensity have been developed, e.g. for attenuation or bright band effects. When using reflectivity data, inaccuracies may occur due to a wrong $Z - R$ relation. Dual-polarisation radars provide promising techniques to overcome most of this inaccuracies.

For hydrological application, the use of radar derived precipitation intensity data is limited as well as the use of accumulation data which are usually needed. The processing of rainfall accumulation fields from subsequent intensity data samples is subject to another inaccuracy which is dependent mainly on the horizontal resolution of the radar data and the time step between the data samples.

Conventional accumulation algorithms usually just add up the subsequent intensity data, multiplied with the time step. This means, for each horizontal grid point, the precipitation accumulation A is calculated with

$$A = \sum_i R_i \Delta t_i \,, \tag{1}$$

where R_i is the precipitation intensity at the time t_i, and Δt_i is the time step.

With Eq. (1) being used, the precipitation intensity is assumed to be constant at each horizontal grid point during the time between subsequent precipitation samples. This does not take into account the movement and development of precipitation systems. For example, a small rain cell passing a grid point just within the time step between two subsequent samples would be lost completely at that point. The inaccuracies of this method increase with the time step Δt_i and are larger for small-scale fast-moving precipitation systems than for stratiform rain.

Figure 1 shows an example how the inaccuracies are reduced using shorter time steps. The images show radar derived 75-minutes precipitation accumulations by adding up the rainfall intensities according to Eq. (1). The rainfall intensities were derived from C-Band reflectivity data using a $Z - R$ relation of $Z = 200R^{1.6}$. (This frequently used $Z - R$ relation is often referred to as "Marshall-Palmer", e.g. in Battan (1973); however the equations presented in Marshall and Palmer (1948) result in a slightly different relation of $Z = 295R^{1.47}$.) During the observation period, several showers crossed the radar area from Southwest to Northeast.

In Fig. 1a, a time interval of 15 minutes was selected. The result are random distributed small areas with high precipitation amounts surrounded by almost echo-free regions. For the image of Fig. 1b, more than twice the data samples were taken using a time step of 6 minutes. Now the propagation path of different rain cells can be anticipated, but several

Correspondence to: R. Hannesen
(R.Hannesen@gematronik.com)

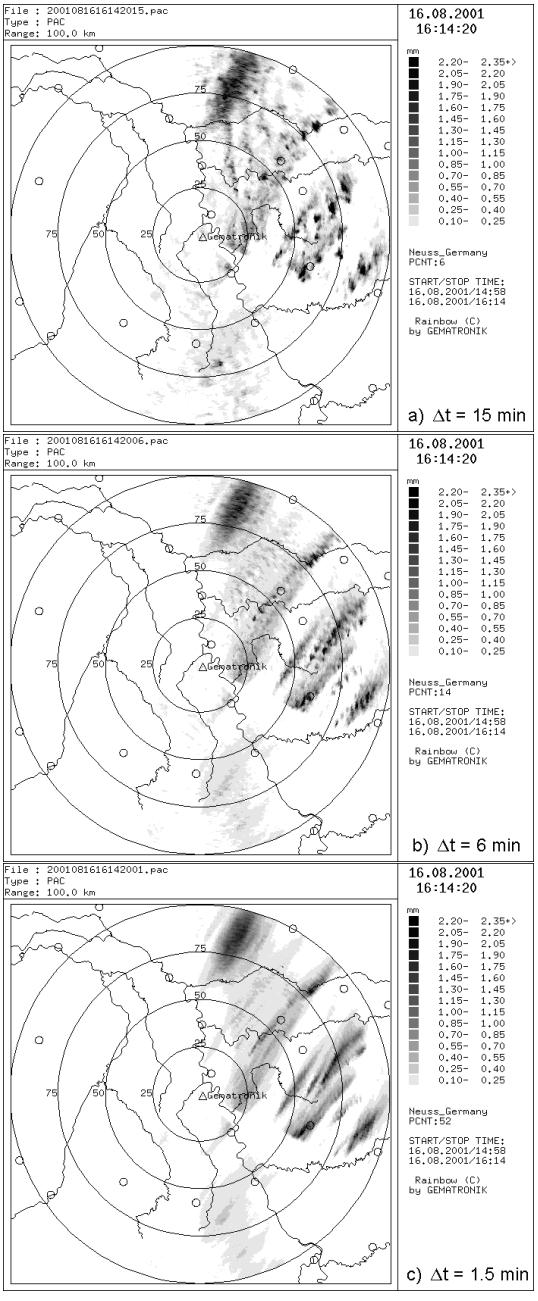

Fig. 1. Radar derived 75-minutes precipitation accumulation assuming constant rainfall intensity during each time step Δt. (a) Δt = 15 min, (b) Δt = 6 min, (c) Δt = 1.5 min.

regions with high and low precipitation alternate along the paths. In the last case (Fig. 1c), the time between the data samples was only one and a half minutes. The result is a good reflection of the real precipitation swaths.

Due to other operational requirements, scan repetition times as short as about one minute are rarely possible. Instead, time steps of 10 or 15 minutes are more common. In such cases, the precipitation accumulation algorithm should take into account the movement and development of precipitation systems between subsequent data samples. A corresponding algorithm is described in this paper.

2 Algorithm description

The combination algorithm for radar data precipitation accumulation consists of two step. First, a movement vector field is derived for a radar data sample, using different techniques. In a second step, the movement information is used to simulate the precipitation system development between two subsequent radar samples.

2.1 Movement vector derivation

In the first step, the movement vectors of the precipitation systems have to be derived. Using radar data, this can be done by one of the following method:

- Cell centroid tracking algorithm. This methods provides one vector for each identified precipitation cell center.
- Cross-correlation tracking algorithm. For that method, the radar area is subdivided into equally-spaced subarrays, and one vector is resulting for each sub-array.
- Volume velocity processing (VVP, cf. Waldteufel and Corbin, 1979) using Doppler radar data. One global movement vector is derived from the horizontal VVP winds of low-tropospheric levels.
- Uniform wind technique (UWT, cf. Persson and Andersson, 1987) using Doppler radar data. For an equally-spaced grid in a low-tropospheric level, horizontal wind vectors are derived.

The latter two methods must be used with some caution for the fact that the moving vector of precipitation echoes is not necessarily identical with the wind vector derived from Doppler data.

For the cross-correlation technique, it can be chosen between optimising for the following parameters: correlation coefficient, mean absolute difference, standard deviation, square mean root, and Canberra metrics (cf. Zgonc and Rakovec, 1998).

The cell centroid tracking algorithm identifies regions, where a user-configured intensity threshold is exceeded, as precipitation cells and correlates the cell centers of subsequent samples.

Finally one (global) or more movement vectors can be specified by user or can be taken from other data sources. This technique however is convenient rather for offline case studies than for real-time application.

For each horizontal grid point P of the radar area, a movement vector $\boldsymbol{v}_P = (u_P, v_P)$ is calculated from interpolation of the above derived vectors.

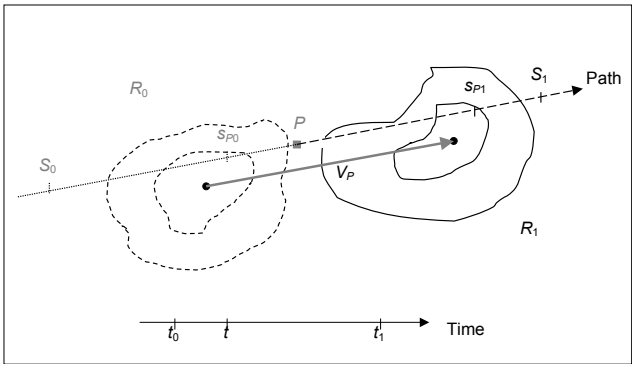

Fig. 2. Schematic sketch of the accumulation step. A precipitation system passes a horizontal grid point P. Precipitation contours from the previous data sample (R_0; dashed, grey) and the actual sample (R_1; solid, black) are indicated. V_P denotes the movement vector for P.

2.2 Accumulation step

The precipitation accumulation step for the time interval between two subsequent radar data samples (at times t_0 and t_1) combines for each horizontal grid point P the corresponding movement vector $\boldsymbol{v}_P$ with the precipitation intensity fields $R_1(x, y, t_1)$ of the actual data sample and the field $R_0(x, y, t_0)$ of the previous sample. For the grid point P, the precipitation accumulation A_P is

$$A_P = \int_{t_0}^{t_1} R(x_P, y_P, t)dt, \tag{2}$$

with $R(x_P, y_P, t)$ being the precipitation intensity at P at the time t. $R(x_P, y_P, t)$ is not known and must be calculated from the measured precipitation intensities R_0 and R_1 at the corresponding locations $s_{P0} = (x_{P0}, y_{P0})$ and $s_{P1} = (x_{P1}, y_{P1})$, assuming a constant change rate of R:

$$\begin{aligned} R(x_P, y_P, t) &= \frac{t_1 - t}{t_1 - t_0} R(x_{P0}, y_{P0}, t_0) \\ &+ \frac{t - t_0}{t_1 - t_0} R(x_{P1}, y_{P1}, t_1) \\ &= \frac{t_1 - t}{\Delta t} R_0(s_{P0}) + \frac{t - t_0}{\Delta t} R_1(s_{P1}), \end{aligned} \tag{3}$$

with $\Delta t = t_1 - t_0$ being the time interval between the subsequent data samples.

Figure 2 shows the situation schematically. The grid point P and the moving vector $\boldsymbol{v}_P$ (where $V_P = |\boldsymbol{v}_p|$) are indicated. The points s_{P0} and s_{P1} from Eq. (3) belonging to the time t are also given. As one can obtain from the image, all precipitation R_0 from the previous sample along the path from S_0 to P has passed the grid point P. In the same way, all precipitation R_1 from the actual sample along the corresponding path from P to S_1 has passed P.

This means that the integral over the time from Eq. (2) can be replaced by an integral over the path by substituting (3) into (2), which yields an equation with known quantities:

$$\begin{aligned} A_P &= \frac{1}{V_P} \int_{S_0}^{P} \frac{s - S_0}{\Delta s} R_0(s)ds \\ &+ \frac{1}{V_P} \int_{P}^{S_1} \frac{S_1 - s}{\Delta s} R_1(s)ds \end{aligned} \tag{4}$$

For this step, we used the following relations:

$$\begin{aligned} dt = \frac{1}{V_P} ds;\ V_P = \frac{\Delta s}{\Delta t};\ \frac{t_1 - t}{\Delta t} = \frac{s_{P0} - S_0}{\Delta s};\\ \frac{t - t_0}{\Delta t} = \frac{S_1 - s_{P1}}{\Delta s} \end{aligned} \tag{5}$$

with $\Delta s = S_1 - P = P - S_0$. For numerical integration, the integral of (4) is replaced by a sum with a step width δs equal to the data resolution; typically a few hundred meters.

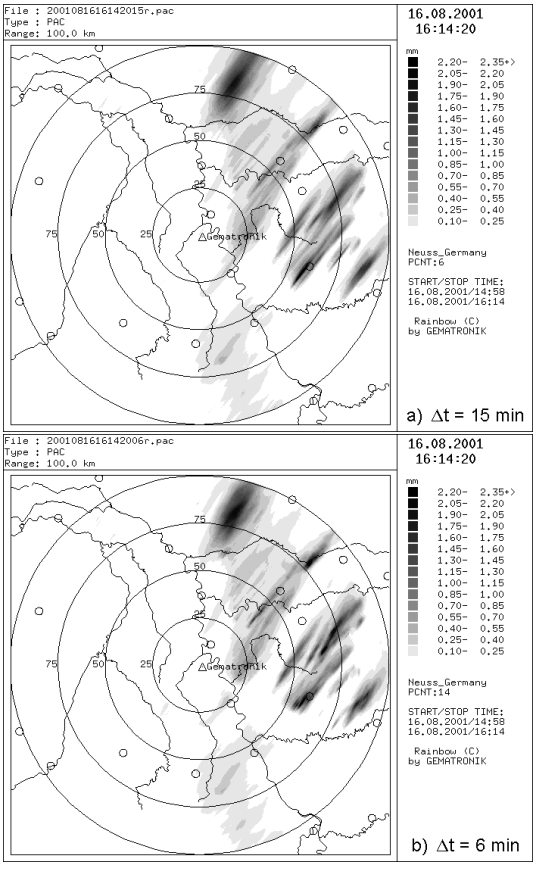

Fig. 3. Radar derived 75-minutes precipitation accumulation by combining the precipitation intensity data using cross-correlation tracking. (a) Time step Δt = 15 min, (b) Δt = 6 min. The improvement compared to Fig. 1 is obvious.

3 Results

3.1 Radar precipitation accumulation

The combination algorithm was first applied on the precipitation intensity data which were used for the example of the

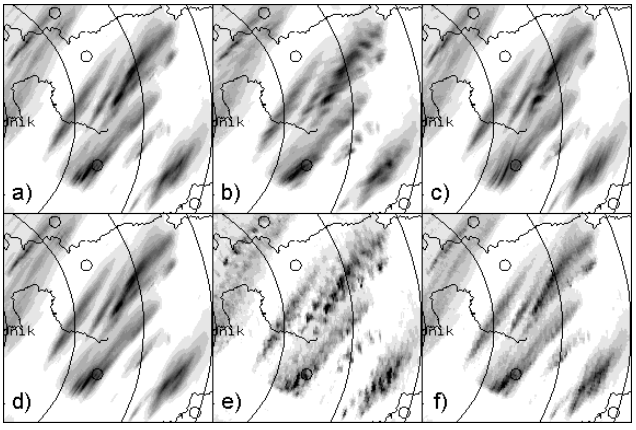

Fig. 4. Radar derived precipitation accumulations with a time step Δt = 6 min (except for case (f), where Δt = 1.5 min); using (a) cross-correlation tracking, (b) VVP wind vectors, (c) UWT wind vectors, (d) constant global vector, (e) and (f) conventional algorithm.

introduction. Figure 3 shows the results of the 75-minutes precipitation accumulation using cross-correlation tracking. For the results of Fig. 3a, a time step of 15 minutes was chosen (same as for Fig. 1a), and for Fig. 3b a time step of 6 minutes (same as for Fig. 1b). One can see that in both cases the resulting accumulations are good representations of the real precipitation swaths. Some short-time developments, however, are missed when using a time step of 15 minutes. The accumulation using a 6 minutes time step thus shows more structured details, and the consistence with that one of Fig. 1c, where a time step of 1.5 minutes had been used, is better.

The accumulation distribution resulting from the combination algorithm does not only depend on the time step, but also on the method with which the movement vector information was obtained. Figure 4 presents image sectors for different vector derivation methods. In each case, a time step of 6 minutes was used (except for Fig. 4f). Figure 4a shows a sector from Fig. 3b, i.e. the accumulation was derived using cross-correlation tracking. The accumulation data of Fig. 4b result from VVP wind vectors, and of Fig. 4c from UWT wind vectors. The data of Fig. 4d were obtained using a constant, global vector for all time steps. For comparison, Figs. 4e and f show results using the conventional algorithm mentioned in the introduction; for Fig. 4e, the time interval was 6 minutes as in cases (a)–(d), and for Fig. 4f it was 1.5 minutes.

The cross-correlation combination (Fig. 4a) provides good results compared to the short-time interval accumulation (Fig. 4f). Good results were also obtained using UWT wind vectors (Fig. 4c) and using a constant global vector (Fig. 4d). The reason for that is the quite homogeneous wind field with a southwesterly flow in mid-tropospheric levels. Therefore, the precipitation systems were propagating more or less with a constant moving vector. The accumulation derived using VVP wind vectors (Fig. 4b), however, provides not so good results. This was caused by the fact that for the data samples

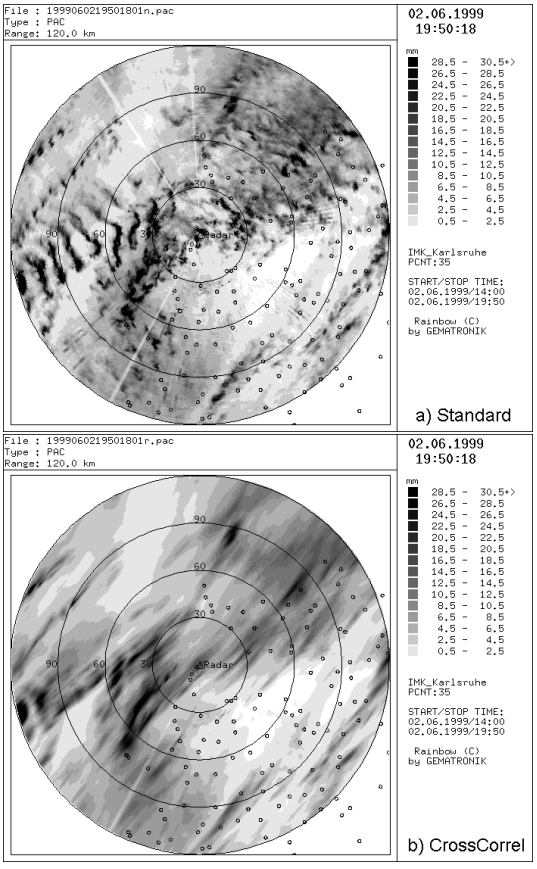

Fig. 5. Radar derived precipitation accumulations of a 6-hours case study with summertime thunderstorms. Time step Δt = 10 min. (a) conventional accumulation, (b) combination algorithm using cross-correlation tracking. Locations of rain gauges are indicated by small circles.

of the later parts of the sample period, only low-level clear-air echoes were available in the vicinity of the radar selected for VVP analysis; and in the boundary layer the flow was rather westerly giving wind vectors different from the precipitation system movement. This example demonstrates that velocity information has to be used with caution for radar echo pattern tracking.

3.2 Comparison with rain gauges

In another case study, the precipitation accumulations derived from a C-Band radar were compared with ground-based data from a rain gauge network. The analysis sample covered a period of 6 hours of a summertime thunderstorm situation. During this time, radar precipitation intensity data were available with a time step of 10 minutes. Figure 5 shows the accumulation data (a) using the conventional algorithm, and (b) using cross-correlation tracking. The locations of the rain gauges are indicated by small circles. As discussed above, the conventional algorithm leads to a clustering (Fig. 5a), whereas the cross-correlation technique provides an accumulation field with cell paths oriented mainly

Table 1. Mean bias factor, root mean square error and correlation coefficient for comparisons of the radar derived accumulations with rain gauge data

Parameter	Accumulation algorithm			
	Conventional	Cross-correlation	VVP wind vectors	UWT wind vectors
Mean bias factor	1.02	0.88	0.87	0.88
Root mean square error	1.15	0.83	0.80	0.82
Correlation coefficient	0.48	0.61	0.64	0.62

from Southwest to Northeast (Fig. 5b).

When the radar derived accumulation data are compared with rain gauge measurements, one can see that the differences between them are smaller in the case of the combination algorithm than for the conventional way (see Fig. 6). A perfect correlation between radar and rain gauge data is not reached, but cannot be expected due to e.g. uncertainties of the $Z - R$ relation and large horizontal gradients of the rain intensity. Table 1 lists the mean bias factor (sum of radar data divided by sum of rain gauge data), the root mean square error (normalised to rain gauge average) and the correlation coefficient for the comparison of radar data derived precipitation accumulation with the corresponding rain gauge measurements. It can be noticed that all combination techniques provide an improvement of the radar data precipitation accumulations: the correlation coefficient is increased and the root mean square error is reduced compared to the conventional algorithm. The mean bias factor, on the other hand, changes from 1.02 for the conventional algorithm to values about 0.88, which means for the combination techniques a slight under-estimation of the radar data compared to the rain gauge values. This effect can be explained by a few locations with unrealistically high radar data accumulations for the conventional algorithm.

For some rain gauges, the improvement is extraordinary. Figure 7 shows enlarged sub-sectors from Fig. 5. The precipitation in mm measured at the different rain gauges (indicated by circles) are also given. One can see that for the conventional case (Fig. 7a), the radar derived accumulations are for some rain gauges ('KN', 'KW', 'Ne' and 'Wi') much too small, and for some others ('Eg', 'Ep') much too large. Using the combination algorithm, the radar data are matching much better (Fig. 7b).

3.3 Computation time statistics

The combination algorithm for radar data precipitation accumulation can be applied real-time on standard PCs or workstations. This is demonstrated by the figures from Table 2, where the corresponding data are given for calculations on a 400 MHz Pentium II PC station of one-hour periods of the presented case studies, i.e. for radar data images of 500 $\times$ 500 pixels with a resolution about 0.5 km. The conventional accumulation algorithm according to Eq. (1) takes very few time: about 1 minute at most (for a one-hour period of 1.5-minute time steps). The cross-correlation technique needs the most CPU time (several minutes for the one-hour period), but in all cases less than about one quarter of an hour, which

Table 2. CPU statistics for the combination algorithm of a one-hour accumulation (400 MHz Pentium II PC). CPU times for the different steps of the algorithm and total times are given. An asterisk * at a number denotes that this value is highly variable depending on the weather situation

Algorithm step	CPU times [seconds] for a one-hour accumulation with time intervals Δt of		
	15 minutes	6 minutes	1.5 minutes
Precipitation intensity from reflectivity	10	20	60
Accumulation step (conventional)	1	2	5
Vector derivation: cross-correlation	240*	300*	450*
Vector derivation: centroid tracking	4	10	35
Vector derivation: VVP wind vectors	10	25	90
Vector derivation: UWT wind vectors	5	12	50
Combination step accumulation	60*	80*	120*
Total: conventional method	**11**	**22**	**65**
Total: cross-correlation	**310***	**400***	**630***
Total: centroid tracking	**74***	**110***	**215***
Total: VVP wind vectors	**80***	**125***	**270***
Total: UWT wind vectors	**75***	**112***	**230***

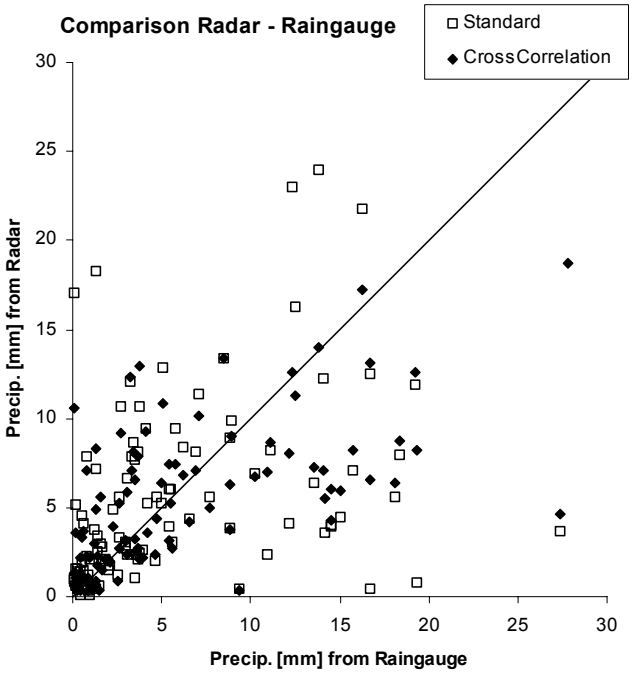

Fig. 6. Scattergram of radar derived precipitation versus corresponding rain gauge data for the gauges indicated in Fig. 5. Open squares for conventional radar data accumulation, solid rhombuses for combination algorithm using cross-correlation tracking. The 1:1 matching line is also given.

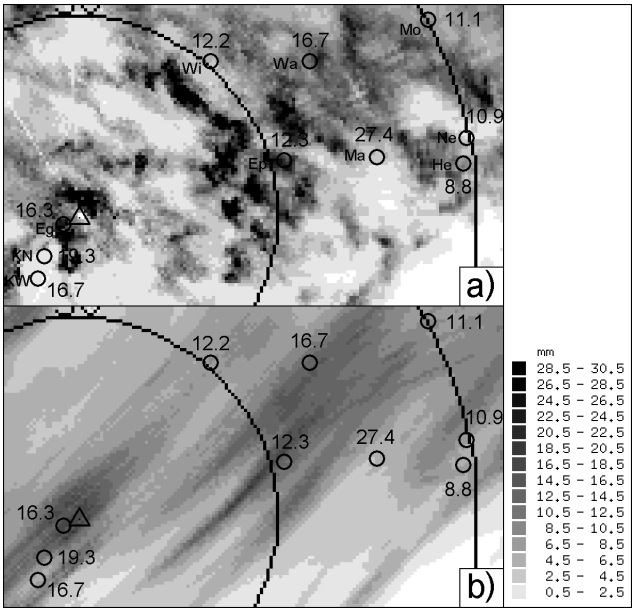

Fig. 7. Radar derived precipitation accumulations (sub-sectors from Fig. 5). (a) conventional accumulation, (b) combination algorithm using cross-correlation tracking. Locations of rain gauges are indicated by circles, rain gauge name abbreviations by characters. The precipitation in mm measured at each rain gauge is also given.

would mean less than 25 per cent average CPU load in case of real-time application. This means that the algorithm can be applied real-time even on machines slower than a 400 MHz PC.

It has to be noted that in general all CPU times are strongly dependent on the data image size. Some processing steps' CPU times additionally depend on the weather situation, in particular on the movement speed. This concerns mainly the cross-correlation tracking and the combination step. For the combination step, it can be obtained from Eq. (4) that the CPU time increases with the path length of integral, which is directly proportional to the propagation speed of the precipitation patterns. The corresponding times are denoted with an asterisk in Table 2.

4 Summary and conclusions

A precipitation accumulation algorithm was presented which combines precipitation intensity data of two subsequent radar data samples with vector information to simulate the movement and development of precipitation patterns in the time between radar samples. For the derivation of movement vectors, different techniques have been presented.

The algorithm provides a significant improvement compared to the conventional method which just adds up precipitation intensities multiplied with the time step. In a case study, the results from the different techniques were compared with rain gauge measurements. In all cases, the correlation coefficient was increased and the root mean square error was reduced compared to the conventional algorithm. The CPU time consumption depends on the algorithm type and on the weather situation. For the selected case studies, the average CPU load on a 400 MHz PC would in all cases be much less than 25 per cent for a real-time application of the algorithm.

For hydrological applications, radar derived precipitation accumulations are often adjusted with rain gauge data. This should not be done for conventional accumulation algorithms, because the errors of this methods are too large to allow further quantitative analysis. Instead, accumulations derived by combination algorithms should be adjusted.

Acknowledgement. The authors would like to thank the Landesanstalt für Umweltschutz Baden-Württemberg (State Institute for Environmental Protection) for providing the rain gauge data.

Part of this work was sponsored by the European Commission in the frame of the MUSIC project (http://www.geomin.unibo.it/orgv/hydro/music/), which is a research project supported by the European Commission under the Fifth Framework Programme and contributing to the implementation of the Key Action "Sustainable Management and Quality of Water", under Contract No. EVK1-CT-2000-00058. The paper does not represent the opinion of the European Community and the Community is not responsible for any use that might be made of data appearing therein.

References

Battan, L.J. (1973): Radar observations of the atmosphere. Univ. of Chicago Press, Chicago, 323 p.

Marshall, J.S. and W. McK. Palmer (1948): The distribution of raindrops with size. J. Meteor. 5, 165–166.

Persson, P.O.G. and T. Andersson (1987): A real-time system for automatic single-Doppler wind field analysis. Proc. Sympos. Mesoscale Analysis and Forecasting, Vancouver, ESA Publication SP-282, 61–66.

Waldteufel, P. and H. Corbin (1979): On the analysis of single-Doppler radar data. J. Appl. Meteor. 18, 532–558.

Zgonc, A. and J. Rakovec (1998): Time extrapolation of radar echo patterns. Proc. COST 75 seminar, Locarno, Switzerland, 23 to 27 March 1998, 229–238.